11th International Conference on Fracture Mechanics of Concrete and Concrete Structures
FraMCoS-11
J. M. Chandra Kishen, A. Ramaswamy, S. Ray and R. Vidyasagar (Eds)
https://doi.org/10.21012/FC11.092359

NUMERICAL INVESTIGATION ON INTERLAYER AND FILAMENT FRACTURE BEHAVIOUR OF 3D PRINTED CONCRETE(3DPC)

PRADEEP S[*], ANANTH RAMASWAMY[†]

[*] Research Scholar, Department of Civil Engineering, Indian Institute of Science (IISc), Bangalore, India
e-mail: pradeeps1@iisc.ac.in

[†] Professor, Department of Civil Engineering, Indian Institute of Science (IISc), Bangalore, India
e-mail: ananth@iisc.ac.in

Key words: 3D printed concrete, Interlayer fracture, Printing time interval, Cohesive zone model, Scalar damage model, Finite element method

Abstract: Concrete additive manufacturing is a recent emerging technology used to complete the construction through layer upon-layer deposition process. Unlike conventionally cast concrete, this automated process introduces distinct interlayers between successive layers, which leads to 3D-printed concrete as anisotropic material. As concrete is a quasi-brittle material and prone to fracture, it is essential to study the effect of the additive manufacturing process on the fracture behavior of 3D-printed concrete. This study uses a finite element simulation approach to examine the interlayer and filament fracture behavior of 3D-printed concrete. A scalar damage model based on isotropic continuum damage mechanics theory, is adopted to describe the failure and damage of the material, and a bilinear traction separation law-based cohesive zone model is used to account for the effect of interlayer bond characteristics of 3DPC. The printing time interval, a deposition time gap between two consecutive layers, is one of the leading printing parameters which control interlayer bond properties of 3D printed concrete. This study elucidated the impact of printing time intervals: 0 mins, 5 mins, and 10 mins on the late age load versus crack mouth opening displacement (CMOD) relation of 3DPC materials with notch locations at interlayer in one set of specimens and at filament in another set of specimens. These simulation results have good agreement with the corresponding experimental results. Further, these simulation results match the experiments at different stages of process: (1) The peak load in the interlayer notch specimen was lower than the filament notch specimen for a particular printing time interval. (2) The peak load decreases as the printing time interval increases for a particular notch position.

1 INTRODUCTION

In recent decades, the construction industry has focused on Concrete additive manufacturing, also known as 3D printing, due to its various advantages like no formwork, cost-effectiveness, and reduced construction time over conventionally cast concrete [1]. One of the significant advantages of this layer-by-layer building process is to allow construction in harsh and less accessible conditions. The possibility of making complex structural geometries using this process further attracts researchers to achieve remarkable mechanical properties of concrete by imitating bio-inspired structures design ([1],[2]). However, unlike conventional concrete, the layer-by-layer automated process makes 3D printed concrete(3DPC) an anisotropic material.

The following four key attributes [3] are essential in the aspects of printability of concrete (1) Extrudability - the ability of pumping and extrusion of concrete, (2)

Buildability - the number of deposited layers without plastic collapse or elastic buckling, (3) Interlayer bonding - the bond between two subsequent layers; and (4) Open time - Available printable time of concrete. The interlayer bonding is the primary key attribute of 3DPC as per fracture aspects, which depends on the printing time interval. Understanding the effect of the printing time interval is crucial since additive manufacturing of large-scale structural components leads to a longer printing time gap between layers, which further affects the interlayer property of 3DPC. For example, the 3D printed pedestrian bridge [4] contained printed elements (3440 mm x 1000 mm x 920 mm) in Gemert, The Netherlands, the total optimum print path length of 25.1 m with a printing speed of 80 mm/s leads to a printing time gap of approximately 5 min and 14 sec between layers. The 2-story residential building [5] printed by COBOD International in Denmark had a printing time gap between 5 min to 15 min between layers. More printing time interval between adjacent layers leads to the famous "cold joint" problem, and less time gap leads to poor buildability of concrete. So, an Optimum printing time interval is essential to improve pre-and post-printing performance of 3DPC.

Due to these interlayer effects, the mechanical behaviour of 3DPC under loading in the printing direction (i.e., loading direction parallel to interlayer) differs from the one perpendicular to the printing direction ([6],[7]). The differences in concrete properties due to lag in the placement of layers introduce differences in the fracture properties of concrete at different layers. Similarly, the fracture characteristics of the notched 3DPC specimen, such as fracture toughness, fracture process zone, load vs. crack mouth open displacement (CMOD), etc., are based on the printing time gap between layers and notch locations (in a filament or an interlayer). As concrete is a quasi-brittle material and prone to fracture, it is essential to understand the effect of the stacking process on the fracture behaviour of 3D-printed concrete.

Existing studies ([7],[8],[9]) focused on the experimental work on the mechanical and fracture behaviour of hardened 3DPC. However, only a few studies have paid attention to the numerical prediction of fracture behaviour of 3DPC. Hence, continuum damage theory alone may not be sufficient to capture the effect of interlayer behaviour of 3DPC. This study focuses on the finite element method implementing scalar damage theory with a bilinear traction separation law-based cohesive zone model to predict fracture characteristics of 3DPC over different printing time gaps and notch positions and further validated with experiments.

2 CONSTITUTIVE MODEL

Concrete is idealized as homogeneous and isotropic material. A continuum damage mechanics-based theory [10] is used to describe the failure and damage of the material. The interlayer between adjacent layers is modelled using bilinear traction separation law-based cohesive zone model [11].

2.1 Scalar damage model

In this model ([10],[12],[13],[20]), The damaged stress tensor is computed from undamaged stress tensor as given in Eq (1),

$$\sigma = (1 - d)D : \varepsilon \tag{1}$$

Here, D is Constitutive elastic stiffness tensor, ε is strain tensor and d – Scalar damage variable which represents failure under homogeneous strain condition varies from 0 for undamaged state to 1 for fully damaged state. The damage evolution is governed by an equivalent strain $\varepsilon_{eq} = \sqrt{\sum_{i=1}^{3} \langle \varepsilon_i \rangle^2}$, where ε_i – principal strain in i^{th} direction.

To consider the damage due to both compression and tension, the total damage variable is taken as a combination of compression and tension ([10],[12],[13]).

$$d(\omega) = \alpha_t^{\beta} d_t(\omega) + \alpha_c^{\beta} d_c(\omega) \tag{2}$$

In this present study, β – Shear exponent to account for shear response of material is taken as 1. Exponential strain softening [14] is adopted for tensile damage behavior of concrete

and Mazars damage evolution [12] is adopted for compressive damage behavior of concrete as described in Eq (3) and (4).

$$d_t(\omega) = 1 - \frac{\omega_0}{\omega} exp\left(-\left(\frac{\omega-\omega_0}{\varepsilon_f-\omega_0}\right)\right) \quad (3)$$

$$d_c(\omega) = 1 - \frac{\omega_0}{\omega}(1 - A_c) - A_c\{exp(B_c(\omega_0 - \omega))\} \quad (4)$$

$$\alpha_t = \sum_{i=1}^{3} \frac{H_i \varepsilon_{ti} \varepsilon_i}{\varepsilon_{eq}^2} \; ; \alpha_c = \sum_{i=1}^{3} \frac{H_i \varepsilon_{ci} \varepsilon_i}{\varepsilon_{eq}^2} \quad (5)$$

Here, H_i depends on the principal strains [12]: $H_i = 0$ if $\varepsilon_i < 0$, 1 otherwise; ε_{ci} and ε_{ti} are the principal values of compressive and tensile strain. ω is a damage defining parameter which takes largest value of equivalent strain ever reached by material during the entire loading history initialized to $\omega_0 = \sigma_t/E$, where σ_t and E are tensile strength and Young's modulus of material. α_t and α_c are weight coefficients [12] which defines contribution of tensile and compressive type of damage respectively for general loading condition. From Eq (5), one can verify that for uniaxial compression, $\alpha_c = 1, \alpha_t = 0$, $d(\omega) = d_c(\omega)$ and vice versa in tension. A_c and B_c are material parameters which can be found out from uniaxial compressive response. The parameter ε_f in Eq (3) derived from below Eq (6),

$$\varepsilon_f = \frac{G_f}{\sigma_t h_{cb}} + \frac{\omega_0}{2} \quad (6)$$

G_f – Fracture energy per area, h_{cb} – Characteristics element size. The damage loading surface is defined as $f = \varepsilon_{eq} - \omega$ and the state variable ω, follows the Kuhn-Tucker conditions $\dot{\omega} \geq 0$, $f \leq 0$, $\dot{\omega} f = 0$. Crack band regularization ([15],[16]) technique is implemented with the damage model to avoid strain localization, mesh dependency and convergence issues.

2.2 Cohesive zone model (CZM)

Finite element method implementing cohesive zone model ([11],[17]) is employed to understand interlayer and filament fracture behavior of 3DPC. In this study, bilinear traction separation law ([11],[17],[18]) is used to describe displacement based [18] cohesive damage model.

The displacement-based damage model is referred from ([17],[18]) and described from Eq (7) to (10)

$$f = (1 - d)ku \quad (7)$$

$$d = \begin{cases} 0 & , u_{m,max} < u_{0m} \\ \min\left(F^{-1}(u_{m,max}), 1\right) & , u_{m,max} \geq u_{0m} \end{cases} \quad (8)$$

$$u_{m,max} = \max\left(u_m, u_{m,max}^{old}\right); u_m = \|u\| \quad (9)$$

d is the cohesive damage variable, during shearing or crack opening, damage variable grows, until interface of material breaks i.e., $d = 1$. The linear separation evolution function F^{-1} is defined as follows [18],

$$F^{-1}\left(u_{m,max}\right) = \frac{u_{fm}}{u_{m,max}}\left(\frac{u_{m,max}-u_{0m}}{u_{fm}-u_{0m}}\right) \quad (10)$$

u_{0m} – threshold of cohesive damage variable, depends on tensile and shear strength of material. More detailed information can be found in Ref. [17] and [18].

3 RESULTS AND DISCUSSION

Based on the above discussed constitutive theory, a 3DPC notched beam specimen is simulated in two dimensions (2D) under three-point quasi-static loading condition. From available experimental study [9], 3DPC – 1 beam specimen printed with 13 filaments by vertical printing path is considered in this present work. Mix proportion of 3DPC – 1 is given in Table 1. More details regarding printer and test setup, rheology properties, Filament size etc., can be found in Ref. [9]

Table 1: Mix proportion of 3DPC – 1 [9]

Water	*306 kg/m^3*
Cement	*873 kg/m^3*
Silica fume	*88 kg/m^3*
Fly ash	*88 kg/m^3*
Sand	*872 kg/m^3*
SP	*8.7 kg/m^3*

Filament notched beam specimen and interlayer notched beam specimen, as shown in Fig. 1 (b) – (c), are numerically modeled for three different printing time intervals of 0 min, 5 mins, and 10 mins. Compressive strength of concrete is taken from [9]. However, tensile

strength and Young's modulus of concrete is not available in [9]. So, these properties are calculated from IS code provision [19] and listed in Table 2.

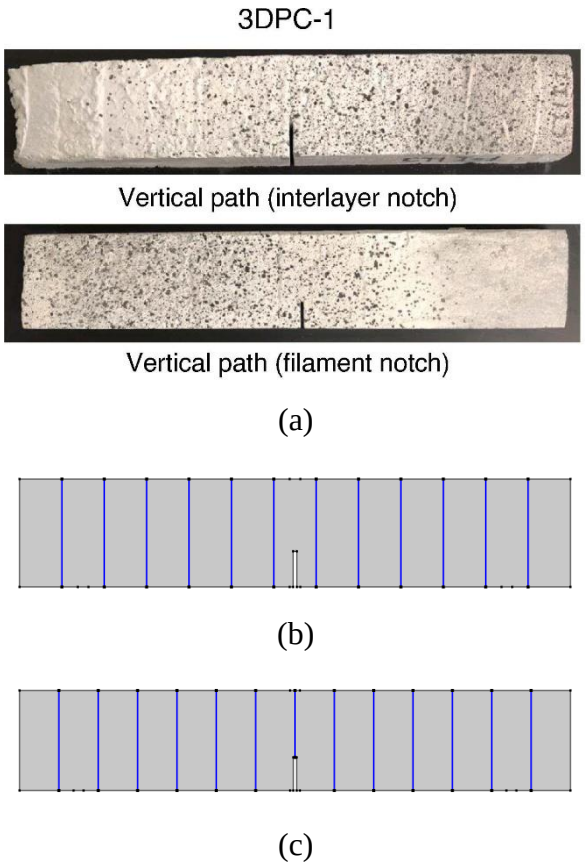

Figure 1: (a) 3DPC – 1 experiment specimens [9] (b) Filament notched beam specimen - simulation (c) Interlayer notched beam modeled specimen - simulation.

Table 2: Material Properties

Compressive strength (f_{ck})	*48.3 MPa*
Tensile Strength (σ_t)	*4.86 MPa*
Young's modulus (E)	*34.8 GPa*
Poisson ratio	*0.21*
Density	*2400 kg/m^3*

In general, the Mazars compression damage parameters (A_c, B_c) are taken from the response of the uniaxial compression test of concrete. Hence, uniaxial test data of 3DPC – 1 is not available in [9], these parameters are calibrated from the range $1 \leq A_c \leq 1.5$ and $10^3 \leq B_c \leq 2 \times 10^3$ as detailed in the study [20] and listed in Table 3. As discussed in Section 2, The cohesive damage variable depends on the interlayer bond strength of 3DPC. However, as per author's knowledge the bond properties of 3DPC – 1 are not available in the literature. In this present work, the interlayer bond strength of concrete such as tensile and shear strength between layers is assumed to be identical. For each printing time interval, these strength parameters are calibrated from the experimental findings of interlayer notched beam specimens and then used to simulate filament notched beam specimens.

Table 3: Scalar Damage model parameters

ω_0	1.3928×10^{-4}
A_c	1.12
B_c	1.555×10^3

Fracture energy per area and interlayer bond strength for each printing time interval is summarized in Table 4. CMOD control loading is used to simulate the fracture behaviour of 3DPC beam specimen. The load vs CMOD plot for filament notched beam specimen corresponding to printing time interval of 0,5, and 10 mins, is as shown in Fig 2(a), 3(a), 4(a) respectively.

Table 4: Fracture energy per area [9] and Interlayer bond strength

		Printing Time Interval		
		0 mins	5 mins	10 mins
Interlayer bond Strength (MPa)		4.25	4.00	2.50
Filament notch	G_f (kN/m)	0.10	0.09	0.085
Interlayer notch	G_f (kN/m)	0.07	0.065	0.06

Similarly, for the interlayer notched beam specimen, the load vs CMOD is plotted and shown in Fig 2(b),3(b) and 4(b). Further, these simulation results are validated with experimental results [9].

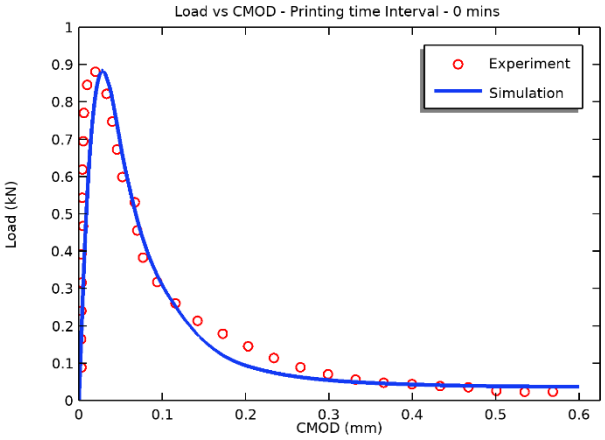

(a)

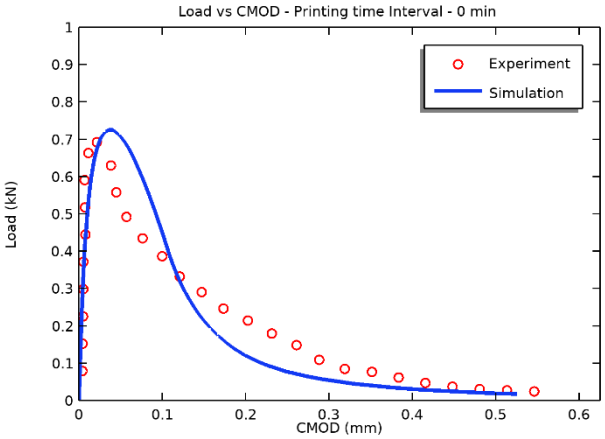

(b)

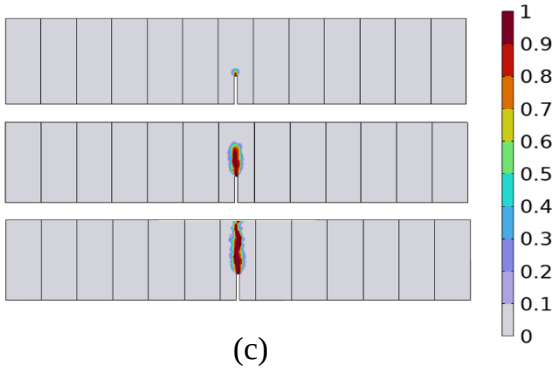

(c)

Figure 2: Simulated load vs CMOD plot for printing time interval – 0 mins (a) Filament notched beam specimen (b) Interlayer notched beam specimen (c) Damage pattern at different stages of process for filament notched beam specimen.

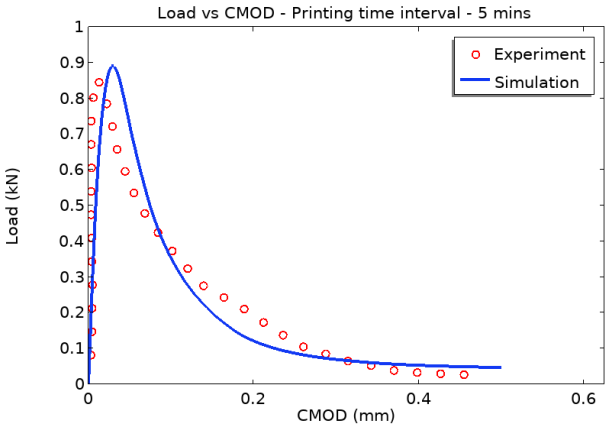

(a)

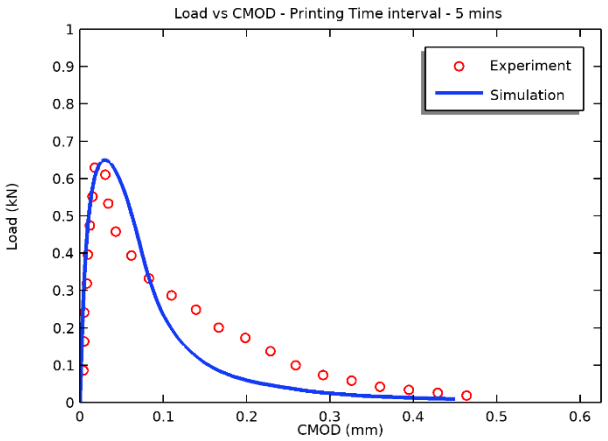

(b)

Figure 3: Simulated load vs CMOD plot for printing time interval – 5 mins (a) Filament notched beam specimen (b) Interlayer notched beam specimen.

The progressive damage pattern from simulated filament notched beam specimen for 0 min printing time interval is shown in Fig 2 (c). This simulated damage pattern is also describing the possible crack path in terms of scalar damage variable d , whose value of 0 represents undamaged part and 1 represents fully damaged part of material.

From these simulation results it was also observed that, (1) the peak loads for interlayer notched beam specimens were generally lower than the filament notched beam specimen and have good agreement with experimental findings [9]. When the printing time interval were 0, 5 and 10 mins, the peak loads for the interlayer notched beam specimen was 19.1 %,

23.1 % and 50 % (In experiment [9], 21.1 %,23.5 % and 48.8 %) lower than those for the filament notched beam specimens.

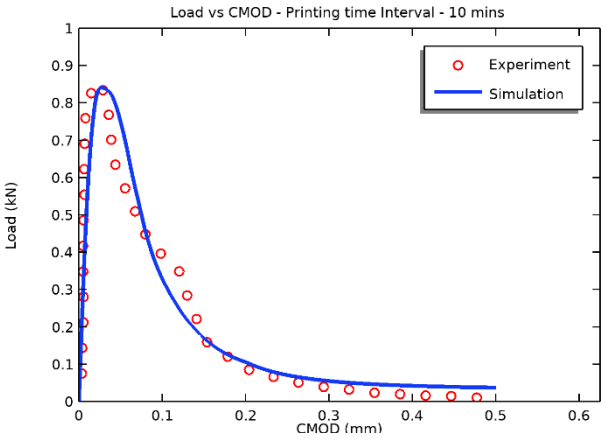

(a)

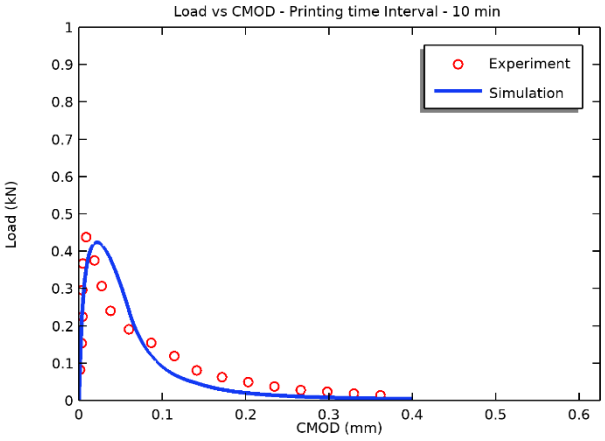

(b)

Figure 4: Simulated load vs CMOD plot for printing time interval – 10 mins (a) Filament notched beam specimen (b) Interlayer notched beam specimen.

(2) As printing time interval increases, the peak load decreases. This effect was more dominant in interlayer notched beam specimen than filament notched beam specimen. For filament notches, the peak loads decreased by 4.01 % and 5.62 % (In [9], 4.44 % and 5.56 %) for 5 min and 10 min specimen compared to 0 min specimen. Similarly for interlayer notches, the peak loads decreased by 9.7 % and 41.7 % (In [9], 8.45 % and 38 %) for 5 min and 10 min specimen compared to 0 min specimen.

4 CONCLUSIONS

In this study, the behavior of 3D printed concrete has been simulated for three different printing time intervals between layers (0 min, 5mins and 10 mins). A finite element method implementing scalar damage model and cohesive zone model is employed to predict the effect of notch position (filament notch or interlayer notch) and printing time interval on the fracture response of 3DPC. In the scalar damage model, the linear combination of Exponential strain softening law and Mazars compression damage evolution law is adopted to describe failure and damage of 3DPC. Bilinear traction separation law based cohesive zone model is adopted to consider the effect of interlayers. CMOD control loading is considered to simulate 2D notched beam specimen under three-point quasi static loading condition. From this study, the followings can be concluded:

- Load vs CMOD curve for different printing time interval is plotted for filament and interlayer notched specimens and further validated with experimental findings.
- The peak loads for interlayer notched beam specimens for a particular printing time interval is lower than the filament notched beam specimen.
- Printing time interval most predominantly affects interlayer fracture behavior than filament fracture behavior of 3DPC. As the time gap between layers increased from 0 min to 10 mins, the peak load decreased by nearly 40 % for interlayer notches and nearly 6 % for filament notches.

REFERENCES

[1] Souza, Marcelo Tramontin, et al. "3D printed concrete for large-scale buildings: An overview of rheology, printing parameters, chemical admixtures, reinforcements, and economic and environmental prospects." Journal of Building Engineering 32 (2020): 101833.

[2] San Ha, Ngoc, and Guoxing Lu. "A review of

recent research on bio-inspired structures and materials for energy absorption applications." Composites Part B: Engineering 181 (2020): 107496.

[3] Soltan, Daniel G., and Victor C. Li. "A self-reinforced cementitious composite for building-scale 3D printing." Cement and Concrete Composites 90 (2018): 1-13.

[4] Salet, Theo AM, et al. "Design of a 3D printed concrete bridge by testing." Virtual and Physical Prototyping 13.3 (2018): 222-236.

[5] Jorgensen, J. (2021, Nov.) "3D Concrete Webinar Series on Advances in Concrete 3D Printing: 3D Printed Construction – Industry Adoption and Future Development". Poster presented at the event of 3DConcrete at the Arizona State University.

[6] Le, Thanh T., et al. "Hardened properties of high-performance printing concrete." Cement and Concrete Research 42.3 (2012): 558-566.*Fract. Mech. of Conc. & Conc. Struct (FraMCoS-6)*, June 17-22, 2006**,** Catania, Italy; pp.1069-76.

[7] Nerella, Venkatesh Naidu, Simone Hempel, and Viktor Mechtcherine. "Effects of layer-interface properties on mechanical performance of concrete elements produced by extrusion-based 3D-printing." Construction and Building Materials 205 (2019): 586-601.

[8] He, Lewei, Wai Tuck Chow, and Hua Li. "Effects of interlayer notch and shear stress on interlayer strength of 3D printed cement paste." Additive Manufacturing 36 (2020): 101390.

[9] Wu, Yun-Chen, and Mo Li. "Effects of Early-Age rheology and printing time interval on Late-Age fracture characteristics of 3D printed concrete." Construction and Building Materials 351 (2022): 128559.

[10] Mazars, Jacky. "A description of micro-and macroscale damage of concrete structures." Engineering Fracture Mechanics 25.5-6 (1986): 729-737.

[11] Yavas, Denizhan, et al. "Fracture behavior of 3D printed carbon fiber-reinforced polymer composites." Composites Science and Technology 208 (2021): 108741.

[12] Mazars, Jacky, and Gilles Pijaudier-Cabot. "Continuum damage theory—application to concrete." Journal of engineering mechanics 115.2 (1989): 345-365.

[13] Arruda, M. R. T., et al. "A modified Mazars damage model with energy regularization." Engineering Fracture Mechanics 259 (2022): 108129.

[14] Jirásek, Milan. "Damage and smeared crack models." Numerical modeling of concrete cracking. Vienna: Springer Vienna, 2011. 1-49.

[15] Bazant, Zdeněk P., and Byung H. Oh. "Crack band theory for fracture of concrete." Matériaux et construction 16 (1983): 155-177.

[16] Jirásek, Milan, and Marco Bauer. "Numerical aspects of the crack band approach." Computers & structures 110 (2012): 60-78.

[17] Geubelle, Philippe H., and Jeffrey S. Baylor. "Impact-induced delamination of composites: a 2D simulation." Composites Part B: Engineering 29.5 (1998): 589-602.

[18] COMSOL Documentation: Contact Analysis Theory (comsol.com)

[19] Bureau of Indian Standards (2000). IS 456: Plain and Reinforced Concrete - Code of Practice. Public.Resource.Org.

[20] Wriggers, Peter, and S. O. Moftah. "Mesoscale models for concrete: Homogenisation and damage behaviour." Finite elements in analysis and design 42.7 (2006): 623-636.